

A Relativistically Expanding Radio Source associated with GRO J1655-40

Jauncey, D.L.¹, Tingay, S.J.^{2,1,3}, Preston, R.A.³, Reynolds, J.E.¹, Meier, D.L.³, Murphy, D.W.³, Tzioumis, A.K.¹, Kesteven, M.J.¹, Lovell, J.E.J.⁴, Jones, D.L.³, Ellingson, S.⁴, Gough, R.¹, McCulloch, P.M.⁴, McKay, D.¹, Migenes, V.¹, Nicolson, G.D.⁵, Sinclair, M.W.¹, and Smits, D.⁵

1. Australia Telescope National Facility (ATNF)
2. Mount Stromlo and Siding Spring Observatories (MSSSO)
3. Jet Propulsion Laboratory (JPL)
4. University of Tasmania
5. Hartebeesthoek Radio Astronomy Observatory (HRAO)

GRO J1655-40 was discovered as a new, bright X-ray source with the BATSE detector of the Gamma Ray Observatory (GRO) on July 27, 1994¹. During the subsequent radio outburst² we completed VLBI synthesis imaging observations at a frequency of 2.29 GHz. An unprecedented angular motion of 65 ± 5 mas day⁻¹ was observed between two components of complex and disparate morphology, or equivalently, an apparent transverse motion of $1.3c \pm_{0.6c}^{0.7c}$ using the likely distance range of 3.5 ± 1.5 kpc as inferred from HI absorption

measurements. This separation rate indicates that the two components were at zero separation near the onset of the radio flare. Similar to the recently reported GRS 1915+105³ it seems that the motion of material ejected from a stellar mass compact object with at least a mildly relativistic velocity may explain the observed radio structural changes in GRO J1655-40. The minimum intrinsic expansion speed of the radio source must be (with minimal assumptions) $0.65c \pm_{0.30c}^{0.18c}$ if the expansion is two-sided, and $0.79c \pm_{0.22c}^{0.11c}$ if one of the two components is a core and the expansion is one-sided. In addition we suggest a possible mechanism by which the radio source was produced, taking into account the X-ray luminosity variability. The two-week delay between the production of radio components and the X-ray outburst may indicate that the X-rays were produced by a super-critical accretion process onto the compact member of this stellar binary system. This process inhibited or smothered the ejection of radio components until the accretion disk stabilised.

Our VLBI images (figure 1) were made from data obtained principally with the SHEVE (Southern Hemisphere VLBI Experiment) VLBI array^{4,5}. The observations span the four days August 21, 22, 23 and 24, beginning approximately nine days after the onset of the radio outburst and reveal two components separated by approximately $0.5''$ which are elongated along the position angle which joins them. Each component shows internal structure. In particular the north-

east component is resolved into three sub-components on the first two days and two sub-components on the final two days. The south-west component is resolved into a bright, compact and variable component with an extension towards the north-east. This extension remains constant in surface brightness and extent over the four day period (to within our errors), but the compact component decreases steadily in brightness. Based on the identification of the north-east sub-components at multiple epochs we estimate that they move with the same speed, relative to the compact component in the south-west. The estimate of the distance to GRO J1655-40 was made possible by comparing the HI absorption profile in the direction of the source (figure 2) to the HI profiles of angularly nearby objects and a consideration of galactic rotation.

The large proper motion we observe for GRO J1655-40 becomes a serious problem when using the standard techniques of synthesis imaging since the source structure changes by a significant fraction of a beamwidth over the twelve hour period of a full observation. Simulations which mimic the observations of moving components have shown that prominent artifacts can be introduced into images, including the spurious bending of features that are in reality linear. In our initial images of the real data (twelve hours duration) we identified artifacts which strongly resembled what we saw in the simulations. Based on the results of the simulations we have imaged only the first five hours of data at each epoch in order to achieve reliable images and separation speeds. A larger synthesised beam is obtained which has its major axis more closely aligned with

the source position angle and in five hours the components separate by 13 mas. Extrapolating the outermost sub-components backwards in time at the observed separation speed we derive the zero separation time of August 13.5 ± 0.5 . This time corresponds to approximately a day after the rapid rise in the radio flux density² and near the end of the decline of the X-ray luminosity (Harmon et al., in preparation).

Two plausible explanations for the source morphology exist. One of the components could be the core, the other component moving relative to it in one-sided expansion. Without astrometric or spectral information we identify the bright, compact and variable south-west sub-component as the core. In this case, and appealing only to the observed apparent speed relative to the speed of light, β_{app} , the minimum intrinsic speed of the north-east component relative to the speed of light, β_{min} , is given by

$$\beta_{min} = \left(\frac{\beta_{app}^2}{\beta_{app}^2 + 1} \right)^{1/2}$$

For $\beta_{app} = 1.3 \pm 0.6$, $\beta_{min} = 0.79 \pm 0.22$. Also for one-sided expansion the maximum angle the motion of the north-east component can make to our line of sight is

$$\theta_{max} = 2 \tan^{-1}(1/\beta_{app})$$

For $\beta_{app} = 1.3 \pm 0.6$, $\theta_{max} = 75^\circ \mp 22^\circ$. Alternatively, if the core lies somewhere between the two components we observe, both components would then be in motion away from a common source and the expansion two-sided. Again only

appealing to the observed apparent motion as the sum of the motion of the approaching and receding components,

$$\beta_{min} = \begin{cases} \beta_{app}/2 & \text{if } \beta_{app} \leq \sqrt{2} \\ (\beta_{app}^2 - 1)^{1/2}/\beta_{app} & \text{if } \beta_{app} > \sqrt{2} \end{cases}$$

For $\beta_{app} = 1.3 \pm_{0.6}^{0.7}$, $\beta_{min} = 0.65 \pm_{0.30}^{0.18}$. Based on the observed apparent motion we can place no constraint on θ_{max} . This scheme assumes only equal and opposite velocities for the two components. Simultaneous ejection is not required and the core can lie anywhere between the two separating components.

The ejection of the radio components twelve days after the X-ray outburst, when the X-ray flux density decreased strongly, is a most peculiar feature of GRO J1655-40. It suggests that the mechanism which formed the X-rays also inhibited jet formation. This can happen in the following way. The luminosity in 2-100 Kev X-rays during the first twelve days of the outburst is of the order of 5×10^{37} ergs s^{-1} - close to or exceeding the Eddington limit for a one solar mass (M_{\odot}) object. The steady (and essentially Eddington) X-ray luminosity suggests that, during the first twelve days, GRO J1655-40 was undergoing a super-critical accretion event. \dot{M} is the accretion rate.

$$\dot{M} > \dot{M}_{EDD} = 10^{18} gs^{-1}(M/M_{\odot})$$

One promising model for producing jets from accretion events is the Blandford-Payne mechanism^{6,7}, which relies on magnetic processes in thin accretion disks. These jets become fast and highly collimated in only a few tens of dynamical

times⁸ (\sim A few ms for a neutron star or black hole). However, a super-critical disk will produce a thick, unstable, radiation-pressure-supported torus in the disk center with a radius of $\sim 10^6 \text{cm} (\dot{M}/10^{18} \text{gs}^{-1})^{9,10,11,12}$. The existence of such a torus could inhibit jet production by either altering the disk and magnetic field geometry (such that a jet does not form in the inner disk) or by enveloping and smothering the jet before it can gain speed. Only when the accretion rate decreases below \dot{M}_{EDD} does the disk become thin in the inner portion, allowing a jet to form via the Blandford-Payne mechanism. The temperature of this accretion torus should be between 10^8 and 10^9 K (9-90 keV) for α the disk viscosity parameter between 0.01 and 1.0^{9,13}. The softening of the spectrum during the initial X-ray outburst and its subsequent hardening during the first twelve days are also consistent with super-critical accretion. This unusual behaviour is associated, respectively, with the waxing and waning of an optically thick, essentially spherical, radiation-pressure-driven wind emerging from the torus surface¹³. A subsequent X-ray and radio outburst (Paciesas et al., personal communication) seems to support this model, as the X-ray luminosity in the 40-430 keV energy range reached only half the level of the initial outburst, and the radio outburst followed more closely. Monitoring the relative timing of future X-ray and radio outbursts as a function of the X-ray luminosity of GRO J1655-40 would further allow this model to be tested.

The identification of relativistically expanding radio jets in GRO J1655-40, along with similar jets in GRS 1915+105, SS433¹⁴ and Cyg X-1¹⁵ indicate

that such behavior may not be uncommon in close binary systems containing a compact stellar object. Furthermore, it seems that a continuum of intrinsic jet speeds, presently ranging from $0.25c$ in SS433 to $0.92c$ in GRS 1915+105, may characterize this new class of source. The delay of the emergence of the radio jets until the decline of the X-ray luminosity in GRO J1655-40 may be an important clue to the nature of jet production not only in these objects, but also in the much more luminous and massive objects in active galactic nuclei.

REFERENCES

- 1 Zhang, S.N., Wilson, C.A., Harmon, B.A., Fishman, G.J.,
Wilson, R.B., Paciesas, W.S., Scott, M., and
Rubin, B.C. IAU circular 6046 (1994).
- 2 Campbell-Wilson, D. and Hunstead, R. IAU circular 6052 (1994)
- 3 Mirabel and Rodríguez Nature **46**, 46-48 (1994).
- 4 Jauncey et al. In Very High Angular Resolution Imaging,
ed Robertson, J. and Tango, W. (Dordrecht: Kluwer), p131 (1994).
- 5 Preston et al. In Sub-Arcsecond Radio Astronomy,
ed Davis, R.J and Booth, R.J. (Cambridge: Cambridge University Press),
p428 (1993).
- 6 Blandford, R.D. and Payne, D.G. Mon.Not.R.astr.Soc. **199**, 883-903 (1982).
- 7 Wardle, M.R. and Königl, A. Astr.Astrophys. **410**, 218-238 (1993).
- 8 Meier, D.L., Payne, D.G., and Lind, K.R. In preparation (1994).
- 9 Shakura, N.I. and Sunyaev, R.A. Astr.Astrophys. **24**, 337-355 (1973).
- 10 Begelman, M.C. and Meier, D.L. Astrophys.J. **253**, 873-896 (1982).
- 11 Abramowicz, M.A., Henderson, P.F., and Gosh, P. Mon.Not.R.astr.Soc
203, 323-338 (1983).
- 12 Papaloizou, J.C.B. and Pringle, J.E. Mon.Not.R.astr.Soc **208**,

721-750 (1984).

13 Meier, D.L. *Astrophys.J.* **256**, 681-716 (1982)

14 Vermeulen, R.C., Schilizzi, R.T., Icke, V., Fejes, I., and
Spencer, R.E. *Nature* **328**, 309-313 (1987)

15 Spencer, R.E., Swinney, R.W., Johnston, K.J., and Hjellming, R.M. *Astro-
phys.J.* **309**, 694 (1986).

16 Crawford, Barlow and Blades *Astrophys.J.* **336**, 212 (1989)

Acknowledgements

We would especially like to thank Duncan Campbell-Wilson for his prompt response in announcing the radio detection and the onset of the radio outburst. We also acknowledge the Observatory Directors for allowing these "target of opportunity" observations to be scheduled at such short notice, and the patience of displaced observers. We would also like to thank the Galileo and Voyager projects and the NASA Deep Space Network for making time available at Tidbinbilla and Goldstone. We are grateful to Mike Barlow for bringing extra information on the distance estimate to our attention, and acknowledge useful discussions with Bob Hjellming and Mike Rupin. Part of this research was carried out at the Jet Propulsion Laboratory, under contract to NASA. The Australia Telescope National Facility is operated in association with the Division of Radiophysics by CSIRO. SJT is supported by an Australian Postgraduate Research Award.

FIGURE 1

The four VLBI images at 2.29 GHz. Data were recorded in right circular polarisation with the 2 MHz bandwidth of the MKII system, and correlated at the CalTech/JPL Block II processor. The contour levels are 1,2,4,8,16,24,32,64,80, and 95 percent of the peak flux density in the montage of 0.59 Jy/beam. The images have each been rotated by 42° and shifted vertically only. The restoring beam is $123 \text{ mas} \times 26 \text{ mas}$ with major axis position angle of 72° . The superposed lines indicate the motion of the sub-components relative to the bright, compact and variable sub-component in the south-west. The extent of the extension to the south-west component is indicated by the line following the 8 percent surface brightness contour on each image. The observations included Australian antennas at Tidbinbilla, Parkes, Hobart, Culgoora and Mopra. Antennas were also used in the USA at Goldstone and Mauna Kea, and also in South Africa at Hartebeesthoek. All intercontinental baselines had non-detections and were therefore not used in the images.

FIGURE 2

The HI absorption profile obtained from the Australia Telescope Compact Array. Comparison of this profile against profiles obtained for B1650-405 and the HI region CTB 35A, as well as a dispersion distance for the pulsar PSR 1641-45, most likely places GRO J1655-40 in the distance range $3.5 \pm 1.5 \text{ kpc}$. We note that the lower limit on the distance may be slightly less than 2 kpc (1.9 kpc)¹⁶

(Barlow, M., personal communication).

FIGURE 1

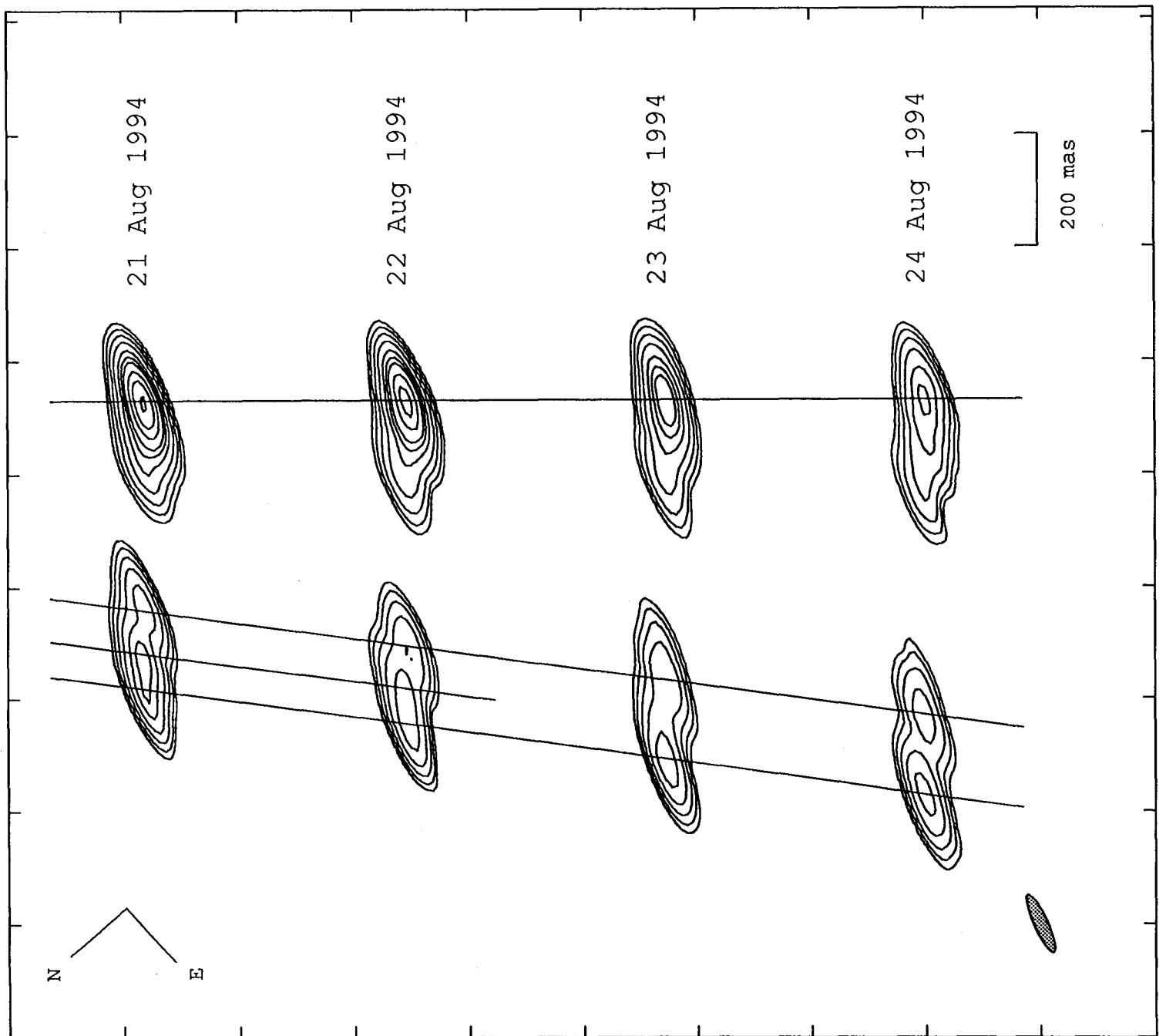


FIGURE 2.

